Multiscale Hydrodynamic Phenomena

M2, Fluid mechanics, MU5MEF15 2021/2022
Friday December 3th, 2021, 8 :30am - 12 :30pm, Room 24.34.107 Part I. : 80 minutes, NO documents

1. Quick Questions In few words and few formula :
1.1 Order of magnitude of drag on a sphere at small Re.
1.2 Order of magnitude of drag on a cylinder at small Re.
1.3 What is the natural selfsimilar variable for Blasius ?
1.4 In which one of the 3 decks of Triple Deck is flow separation ?
1.5 What is the KdV equation ? What balance is it ? One example of solution.
1.6 What is Burgers equation ? What balance is it ? One example of solution.
1.7 ∂'Alembert equation : write the equation and the generic solution of it.
1.8 Quote at least two RER B stations linked with asymptotic modelisation.

2. Exercice
We look at the displacement of a small ball of very small mass in a very viscous flow, in the gravity field. The ball is initially at rest, we look at the position as function of time.
2.1 Show that we obtain the following equation, (of course ε is a given small parameter that you have to define with the parameters of the problem and you have to decide the proper orientation of motion)

$$(E_\varepsilon) \quad \varepsilon y''(t) = -y'(t) - 1 \text{ with } y(0) = 0, \quad y'(0) = 0.$$

We want to solve this unsteady problem with the Matched Asymptotic Expansion method.
2.2 Why is (E_ε) problem singular ?
2.3 What is the outer problem and what is the possible general form of the outer solution ?
2.4 What is the inner problem of (E_ε) and what is the inner solution ? (hint : for the inner problem time is small and displacement y is small as well)
2.5 Suggest the plot of the inner and outer solution.
2.6 What is the exact solution of (E_ε) for any ε. Check that we recover inner and outer solution.
2.7 Comments ?

3. Exercice
Let us look at the following ordinary differential equation : $(E_\varepsilon) \quad \dfrac{d^2y}{dt^2} = -y - \dfrac{\varepsilon}{2}\dfrac{dy}{dt}, \quad$ valid for any $t > 0$ with boundary conditions $y(0) = 1$ and $y'(0) = 0$. Of course ε is a given small parameter.
We want to solve this problem with Multiple Scales Analysis.
3.1 Expand up to order ε : $y = y_0(t) + \varepsilon y_1(t)$, show that there is a problem for long times.
3.2 Introduce two time scales, $t_0 = t$ and t_1, what is the relation between t, t_1 and ε ?
3.3 Compute $\partial/\partial t$ and $\partial^2/\partial t^2$
3.4 Solve the problem.
3.5 Suggest the plot of the solution.
3.6 What is the exact solution for any ε, compare.

4. Exercice
Solve with WKB approximation the problem

$$(E_\varepsilon) \quad \varepsilon y'(x) + 2y(x) = 0 \text{ with } y(0) = 1$$

Compare with exact solution.

empty page

M2, Fluid mechanics 2021/2022
Friday, December 3th, 2021
Part II. : 1h 15 min all documents.

Multiscale Hydrodynamic Phenomena

Film Flow down on a plane : hydraulic jump

This is a part of "Beyond Shallow Water : Appraisal of a numerical approach to hydraulic jumps based upon the Boundary Layer theory" by Vita et al. European Journal of Mechanics / B Fluids 79 (2020) 233-246. We consider the thin film 2D flow on a horizontal plate, see figure 5, and we look at the equation that may explain hydrolic jump (as presented by Higuera in ref [25] "The hydraulic jump in a viscous laminar flow", J. Fluid Mech. 274 (1994) 69-92 and ref [26] "The circular hydraulic jump", Phys. Fluids 9 (5) (1997) 1476-1478.).
As all the results are more or less in the paper, be careful and rigorous to prove the results.

Equations :
1.1 Write incompressible Navier Stokes equations in 2D, eq. (1).
1.2 Write the kinematic condition at the interface, and no slip boundary condition. Which equations are they in the paper ?
1.3 How is the flow for $y > h$ (in air) in terms of pressure ? and in terms of viscosity ? (it is maybe not clearly written in the paper, you must do some extra classical hypothesis).
1.4 Equation (4a,b,c) use c_0 as velocity scale. Use another velocity scale, say U_0, write a version of (4a,b,c) with the Froude number.
1.5 Verify that with an another choice of characteristic velocity $U_0 = c_0$ (i.e. $Fr = 1$) we obtain (5a,b,c).

Toward Saint Venant :
2.1 Starting from (5a,b,c), verify the Prandtl transposition theorem and obtain (7)
2.2 Obtain (8a,b) from (7)
2.3 Give some general properties/ draw backs of Saint Venant equations.

Some solutions of the equations (5a,b,c) not associated with the hydraulic jump :
3.1 In section 4.1 of the paper the solution at the center line of symmetry is $\tilde{z}(3\tilde{z} - 2)/2$. Check it works.
3.2 In section 4.2.1, obtain equation (26),
3.3 Show that (26) has a self similar solution
3.4 In section 4.2.2, same questions.

Some solutions of the equations (5a,b,c) associated with the hydraulic jump :
4.1 Check that with the choice of characteristic velocity $U_0 = Q_0/h_0$, it gives equation 27 (see question 1.4).
4.2 Show that for large Froude, there is no more pressure gradient. Show that we can obtain a self similar solution $\tilde{u} = f(\tilde{y}/\tilde{x})/\tilde{x}$. This is called the "Watson solution".
4.3 Show that for small Froude, there is no inertia. Show that we can obtain a Poiseuille solution .

About the jump :
5.1 Classically the jump is solved using "Bélanger" relations in an ideal fluid framework (in 1D Saint Venant). There is a discontinuity in height and velocity. What is Bélanger equation for a "hydraulic jump" ?
5.2 The change in height that we observe in figure 5 and 6 is the "hydraulic jump", there, we have reintroduced viscosity in a thin layer flow. The Watson (upstream) and Poiseuille (downstream) solutions are connected by a fast change in water depth. We have no more discontinuity but an abrupt change in water depth. Considering the lectures on KdV, what are the next effects that we have neglected and that we must consider next ? What is the associated not so small parameter ?
5.3 Another effect is surface tension, what is the order of magnitude of the stress associated with ?

European Journal of Mechanics / B Fluids 79 (2020) 233–246

Contents lists available at ScienceDirect

European Journal of Mechanics / B Fluids

journal homepage: www.elsevier.com/locate/ejmflu

Beyond Shallow Water: Appraisal of a numerical approach to hydraulic jumps based upon the Boundary Layer theory

Francesco De Vita [a,*], Pierre-Yves Lagrée [b], Sergio Chibbaro [b], Stéphane Popinet [b]

[a] Linné FLOW Centre and SeRC (Swedish e-Science Research Centre), KTH Mechanics, S-100 44 Stockholm, Sweden
[b] Sorbonne Université, CNRS, Institut Jean le Rond d'Alembert, 75005 Paris, France

ARTICLE INFO

Article history:
Received 14 September 2018
Received in revised form 1 July 2019
Accepted 13 September 2019
Available online 19 September 2019

Keywords:
Shallow water
Saint-Venant
Boundary layer flows

ABSTRACT

We study the flow of a thin layer of fluid over a flat surface. Commonly, the 1-D Shallow-water or Saint-Venant set of equations are used to compute the solution of such flows. These simplified equations may be obtained through the integration of the Navier–Stokes equations over the depth of the fluid, but their solution requires the introduction of constitutive relations based on strict hypothesis on the flow régime. Here, we present an approach based on a kind of boundary layer system with hydrostatic pressure. This relaxes the need for closure relations which are instead obtained as solutions of the computation. It is then demonstrated that the corresponding closures are very dependent on the type of flow considered, for example laminar viscous slumps or hydraulic jumps. This has important practical consequences as far as the applicability of standard closures is concerned.

1. Introduction

The "shallow water equations" or "Saint-Venant Equations", from the author of the first proposition [1], are a classical model useful for a large variety of practical configurations in coastal and hydraulic engineering. For example, they are used to predict flows in rivers, in open channels, in lakes, in shallow seas. Floods are simulated with the shallow water equations, as well as tides and many other environmental applications (see for instance Chanson's book [2]). The depth averaging strategy to obtain them is also used for many non-Newtonian flows [3] useful in industrial (concrete) or environmental applications (mud flows, avalanches). Moreover, the Saint-Venant equations are an hyperbolic system analogous to compressible gas flow so that the problem has some universality [4].

Nevertheless, the Saint-Venant equations are based on vertical averaging, which gives rise to several problems as it oversimplifies the physics. One of the approximation comes from the hypothesis of small depth compared to the length of the phenomena. This fundamental hypothesis is not relaxed here, but it is known that if depth increases, dispersive effects appear (the celerity of the waves depends on their wavelength [5]). What will be discussed here is the fact that one needs strong hypothesis on the shape of the velocity profile and on the wall shear stress to close the system of equations. Indeed, the Saint-Venant equations were originally proposed on a phenomenological basis. In [6] an asymptotic analysis is proposed to derive them from the 2D Navier–Stokes equations with mixed boundary conditions. In that derivation, only the laminar case is considered and the derived one-dimensional unclosed equations are closed primarily through a simple constant velocity assumption. Since then, while some attempts have been made to justify the different approximations and to point out more general non-constant closures [7], most often the constant closure is retained in practical computations [8]. All the numerical schemes set the so called Boussinesq coefficient (which accounts for the non-uniform velocity profile in the transverse direction) to one; recently, [9] proposed to artificially increase the Boussinesq coefficient in order to reduce oscillations in transcritical flows or unsteady flows over frictional beds. The influence of the modelling of the wall shear stress has been recently discussed for jumps in water and granular flows, where closure is very different [10].

Furthermore, the range of application of the Saint-Venant model is notably limited because it does not describe the vertical profile of the horizontal velocity. For this reason, the multilayer approach to the Shallow Water equations has been developed, and in particular in the form of numerical schemes for a set of Saint-Venant-like systems. It consist in dividing the liquid depth in layers, each one described by its own height and velocity [11,12], thus modelling the fluid as composed of layers of immiscible liquids. Mass exchanges between layers have also been considered [13–15]. From a numerical point of view, the global stability of weak solutions for the method proposed in [13] has been demonstrated in [16], while new efficient techniques have been recently developed [17–19]. Concerning applications

* Corresponding author.
E-mail address: fdv@mech.kth.se (F.D. Vita).

https://doi.org/10.1016/j.euromechflu.2019.09.010
0997-7546/

beyond Newtonian fluids, a multilayer method with $\mu(I)$ rheology and side walls friction has also been derived [20]. It is important to note that since these multilayer schemes have been developed as mathematical/numerical schemes, less attention has been paid to the physical boundary conditions and the relevant friction coefficients. An alternative method is also worth mentioning, consisting in performing a gradient expansion of the depth-averaged Navier–Stokes equations which gives a system of equations for the depth, the flow rate and an additional variable which accounts for the deviation of the wall shear from the shear corresponding to a parabolic velocity profile [21,22]. This approach has had some success in particular in the analysis of the motion of viscous liquid films.

Here we follow a different path to present an unified picture of the problem. We hope in this way to shed some light on the links between different approaches, which are either more physically or mathematically grounded. Starting from the Saint-Venant model, we would like to address the issue of the value of the Boussinesq coefficient. In order to get information on this coefficient, we deal with a reduced system obtained from the Navier–Stokes equations using an asymptotic thin-layer expansion, which results in fact in the classical boundary layer or Prandtl equations. From a conceptual point of view, it means that the domain may be divided into two physically separated regions: an ideal fluid and a viscous boundary layer [23]. The equations we obtain asymptotically, are actually the same already proposed to tackle the problem of the standing hydraulic jump on phenomenological grounds [24], when considering the limit of infinite Reynolds number. In particular, Higuera [25,26] was the first to use these boundary layer equations to study a viscous hydraulic jump. This is an important test case that we shall repeat in the present work with a different numerical approach.

This simplified set of boundary layer or Prandtl equations will allow to compute directly the shape factor and the wall shear stress, whereas they are parameters in standard Saint-Venant approaches. Indeed, from a practical point of view, one success of the Shallow Water equations is its ability to describe a standing jump. This is known as Bélanger equations [27]. Indeed, as shown by Watson [28], the position of the standing jump within the Saint-Venant description depends on the modelling of viscous effects. Many authors have tried, since then, to understand the structure of the radially-symmetric or 2D hydraulic jump [29–31] using various techniques issued from simplified boundary layer theory [29,32,33]. At the same time, thanks to 2D Navier–Stokes computations, Dasgupta et al. [34] were able to simulate completely the problem, while a similar analysis was performed for a flow over a bump [35]. In this work, we will characterize clearly what is the actual friction in terms of the Boussinesq coefficients in order to assess the validity of the different hypothesis usually adopted together with the Saint-Venant model. Besides, similar closure problems are encountered in different physical phenomena: granular flows when modelled by a Savage–Hutter depth-averaged model [36]; or flows in arteries when modelled by averaging over the circular cross section. Note that the same idea has already been applied for these problems [37–39].

Starting from a physically-sound model, we need a numerical scheme to discretize and simulate it. It turns out that the natural scheme for our model is the one proposed for the multilayer Saint-Venant equations [13,14] with the introduction of an appropriate boundary condition that allows to compute the wall shear stress without the input of friction coefficients. This is fundamental for the proper description of transcritical flows or hydraulic jumps where errors in the quantification of the bottom friction and in the reconstruction of the vertical velocity profile can lead to instabilities or overestimation of the dissipation.

The aim of this paper is thus to present in a general way a theoretical boundary layer model coupled with a versatile numerical model [13,14]. The relation between the boundary layer model and the numerical multi-layer schemes developed for the Saint-Venant equations will therefore be emphasized. The ensemble constitutes a general framework applicable to a wide range of phenomena. For instance, a boundary layer interacting with an external flow may lead to a "jump" in several different contexts [40]: it was first observed by [41] for compressible flows, and has been identified by [42–44] for boundary layer mixed convection flows. This behaviour often corresponds to a "triple deck" structure [45,46]. To support this view, we will recompute the Higuera solution, and we will present several other similar test cases while comparing the numerical solutions with the analytical ones whenever possible. We also discuss in some details the numerical scheme used to solve the equations *via* the free solver *Basilisk* [47].

The paper is organized as follows: in the first section, the Navier–Stokes equations are presented with their thin layer approximation leading to the Reduced Navier–Stokes set, which are Prandtl equations with specific boundary conditions and hydrostatic pressure. This system is integrated over the depth to obtain the Saint-Venant equations. Then, in the second section, the numerical "multilayer technique" is presented to solve the system. In the third section, some viscous slump flows are presented (Huppert slumps), then the Higuera standing jump solution is resimulated. Finally, the influence of a bottom slope on the position of the standing jump is presented.

2. Governing equations

2.1. Navier–Stokes equations

The overall multiphase flow problem of two fluids (say a liquid and a gas) with a separating free surface over a given bottom may be simplified if one of the fluid is much heavier than the other. In this case, free surface flow phenomena can be fully described by the incompressible Navier–Stokes equations for the heavy fluid only, with proper boundary conditions at the interface. For simplicity we will consider a two-dimensional flow with x the horizontal axis and z the vertical axis, pointing upward. The location of the free surface is denoted as $\eta(x,t)$, and the position of the bottom (or bathymetry) is denoted as $z_b(x)$, so that the depth is $h = \eta - z_b$. Across the depth the Navier–Stokes equations can be written as:

$$\frac{\partial \mathbf{u}}{\partial t} + \mathbf{u}\cdot\nabla\mathbf{u} = -\frac{1}{\rho}\nabla p + \nu_0\nabla^2\mathbf{u} + \mathbf{f}, \qquad \nabla\cdot\mathbf{u} = 0, \tag{1}$$

where $\mathbf{u} = (u, w)$ is the velocity field, p the pressure, ν_0 the kinematic viscosity, ρ the mass density ($\mu = \rho\nu_0$ is the dynamic viscosity), and $\mathbf{f} = -g\hat{\mathbf{z}}$ the gravitational force. The two boundary conditions closing the system of Eqs. (1) are the kinematic boundary condition at the free surface

$$\frac{\partial \eta}{\partial t} + u_s\frac{\partial \eta}{\partial x} - w_s = 0, \tag{2}$$

with no tangential stress at the surface and continuity of the normal stress, and the impermeability condition at the bottom (and no slip for viscous flow)

$$u_b\frac{\partial z_b}{\partial x} - w_b = 0. \tag{3}$$

The subscripts s and b denote quantities at the free surface and at the bottom respectively. Let us rescale the Eqs. (1) introducing two characteristic dimensions h_0 (typical depth) and L (a typical evolution length), in the z and x direction respectively, a typical wave amplitude a_s and a characteristic wave speed c_0 =

$\sqrt{gh_0}$. With these quantities we can define two dimensionless parameters:

$$\varepsilon = \frac{h_0}{L} \quad \text{and} \quad \delta = \frac{a_s}{h_0};$$

we do not take into account the possibility of dispersion leading to solitary waves [5,48]. The classical Saint-Venant derivation assumes the characteristic length in the vertical direction z to be smaller than in the horizontal direction, *i.e.* $\varepsilon \ll 1$, and $\delta = \mathcal{O}(1)$ which allows to produce jumps. On the contrary, the Airy linearized wave theory on arbitrary depth requires $\varepsilon = \mathcal{O}(1)$ and $\delta \ll 1$. With the scales defined above it is possible to make dimensionless all the quantities in the Navier–Stokes equations:

$$\tilde{x} = \frac{x}{L} = \frac{\varepsilon x}{h_0}, \quad \tilde{z} = \frac{z}{h_0}, \quad \tilde{t} = \frac{\varepsilon c_0 t}{h_0}, \quad \tilde{u} = \frac{u}{c_0} \quad \text{and} \quad \tilde{w} = \frac{w}{\varepsilon c_0}$$

where scales of time and transverse velocity are chosen assuming that inertial terms are dominant over viscous ones. For pressure, assuming the reference pressure to be zero at the surface, the following scales are taken:

$$\tilde{p} = \frac{p}{\rho g h_0}, \quad \tilde{\eta} = \frac{\eta}{h_0}, \quad \tilde{h} = \frac{h}{h_0},$$

Thus the rescaled system of Navier–Stokes equations is:

$$\frac{\partial \tilde{u}}{\partial \tilde{x}} + \frac{\partial \tilde{w}}{\partial \tilde{z}} = 0, \tag{4a}$$

$$\frac{\partial \tilde{u}}{\partial \tilde{t}} + \frac{\partial \tilde{u}^2}{\partial \tilde{x}} + \frac{\partial \tilde{u}\tilde{w}}{\partial \tilde{z}} = -\frac{\partial \tilde{p}}{\partial \tilde{x}} + \frac{\mu}{\varepsilon \rho c_0 h_0}\left(\frac{\partial^2 \tilde{u}}{\partial \tilde{z}^2} + \varepsilon^2 \frac{\partial^2 \tilde{u}}{\partial \tilde{x}^2}\right), \tag{4b}$$

$$\varepsilon^2\left(\frac{\partial \tilde{w}}{\partial \tilde{t}} + \frac{\partial \tilde{u}\tilde{w}}{\partial \tilde{x}} + \frac{\partial \tilde{w}^2}{\partial \tilde{z}}\right) = -\frac{\partial \tilde{p}}{\partial \tilde{z}} - 1 + \varepsilon \frac{\mu}{\rho c_0 h_0}\left(\frac{\partial^2 \tilde{w}}{\partial \tilde{z}^2} + \varepsilon^2 \frac{\partial^2 \tilde{w}}{\partial \tilde{x}^2}\right). \tag{4c}$$

Note that the topography variations are supposed compatible with the long-wave hypothesis: $\frac{\partial z_b}{\partial x} = \varepsilon \frac{\partial \tilde{z}_b}{\partial \tilde{x}}$. Note as well that the Froude number is one by construction, since we are considering flows with a single velocity scale. The velocity $\tilde{u}$ can still be smaller or larger than one, as a result of the computation.

2.2. Reduced Navier–Stokes equations in the boundary-layer approximation

Since we have assumed that $\varepsilon \ll 1$, Eqs. (4) can be simplified through elimination of the terms of order $\mathcal{O}(\varepsilon)$ and, defining Reynolds number $Re = \varepsilon \rho c_0 h_0/\mu$ which may be large or small (but not smaller than ε), gives:

$$\frac{\partial \tilde{u}}{\partial \tilde{x}} + \frac{\partial \tilde{w}}{\partial \tilde{z}} = 0, \tag{5a}$$

$$\frac{\partial \tilde{u}}{\partial \tilde{t}} + \frac{\partial \tilde{u}^2}{\partial \tilde{x}} + \frac{\partial \tilde{u}\tilde{w}}{\partial \tilde{z}} = -\frac{\partial p}{\partial \tilde{x}} + \frac{1}{Re}\frac{\partial^2 \tilde{u}}{\partial \tilde{z}^2}, \tag{5b}$$

$$0 = -\frac{\partial p}{\partial \tilde{z}} - 1 \tag{5c}$$

This system of equation has the following boundary conditions at the free surface $\tilde{z} = \tilde{z}_b + \tilde{h}(\tilde{x}, \tilde{t})$, namely velocity of interface, reference pressure, and no shear stress:

$$\tilde{w} = \frac{\partial \tilde{\eta}}{\partial t} + \tilde{u}\frac{\partial \tilde{\eta}}{\partial \tilde{x}}, \quad \tilde{p}(\tilde{x}, \tilde{z} = \tilde{z}_b + \tilde{h}(\tilde{x}, \tilde{t})) = 0, \quad \frac{\partial \tilde{u}}{\partial \tilde{z}} = 0, \tag{6}$$

and at the solid bottom $\tilde{z} = \tilde{z}_b$ there is the no-slip boundary condition for both $\tilde{u} = 0$ and $\tilde{w} = 0$. The set of Eqs. (5a)–(5c) are the Prandtl equations for boundary-layer flows, and for this reason we call them Reduced Navier–Stokes Prandtl equations (RNSP). Together with the above boundary conditions, they are the system which we employ in this study.

2.3. RNSP equations with Prandtl transposition theorem

Note that the classical Prandtl transposition theorem may be used here [49]; it consists in changing $\tilde{z}$ in $\tilde{z} - \tilde{z}_b$, while $\tilde{u}$ is unchanged, and $\tilde{w}$ is replaced by $\tilde{w} - \frac{\partial \tilde{z}_b}{\partial \tilde{x}}\tilde{u}$. With this transformation, the no-slip boundary condition is at $\tilde{z} = 0$. The pressure term $-\frac{\partial \tilde{p}}{\partial \tilde{x}}$ changes to (using the chain rule derivative and (5c)):

$$-\left(\frac{\partial \tilde{p}}{\partial \tilde{x}} - \frac{\partial \tilde{z}_b}{\partial \tilde{x}}\frac{\partial \tilde{p}}{\partial \tilde{y}}\right) = -\frac{\partial \tilde{p}}{\partial \tilde{x}} - \frac{\partial \tilde{z}_b}{\partial \tilde{x}}.$$

Hence the momentum equation reads:

$$\frac{\partial \tilde{u}}{\partial \tilde{t}} + \frac{\partial \tilde{u}^2}{\partial \tilde{x}} + \frac{\partial \tilde{u}\tilde{w}}{\partial \tilde{z}} = -\frac{\partial \tilde{p}}{\partial \tilde{x}} - \frac{\partial \tilde{z}_b}{\partial \tilde{x}} + \frac{1}{Re}\frac{\partial^2 \tilde{u}}{\partial \tilde{z}^2}, \tag{7}$$

where $\tilde{z} = 0$ is now the bottom and $\tilde{z} = \tilde{h}$ the free surface.

2.4. Shallow water or Saint-Venant equations

The set of Eqs. (5a)–(5c) can now be integrated over the depth using Leibniz rule and boundary conditions to obtain the system linking the two variables $(\tilde{Q}, \tilde{h})$:

$$\frac{\partial \tilde{h}}{\partial \tilde{t}} + \frac{\partial}{\partial \tilde{x}}\int_{z_b}^{\eta} \tilde{u} d\tilde{z} = 0, \tag{8a}$$

$$\frac{\partial}{\partial \tilde{t}}\int_{z_b}^{\eta} \tilde{u} d\tilde{z} + \frac{\partial}{\partial \tilde{x}}\int_{z_b}^{\eta} \tilde{u}^2 d\tilde{z} = -\tilde{h}\frac{\partial \tilde{h}}{\partial \tilde{x}} - \tilde{h}\frac{\partial \tilde{z}_b}{\partial \tilde{x}} - \frac{1}{Re}\left(\frac{\partial \tilde{u}}{\partial \tilde{z}}\right)_b, \tag{8b}$$

where we recall that $\tilde{h} = \tilde{\eta} - \tilde{z}_b$. The mass flow rate is then

$$\tilde{Q} = \int_{\tilde{z}_b}^{\eta} \tilde{u}\, d\tilde{z}. \tag{9}$$

Thus, a closed 2D problem has been transformed into a not-closed 1-D problem. Therefore, an hypothesis on the shape of the profile is required to obtain a relation between the unknowns ($\int_{\tilde{z}_b}^{\eta} \tilde{u}^2\, d\tilde{z}$, $\frac{\partial \tilde{u}}{\partial \tilde{z}}|_b$) and the variables $(\tilde{Q}, \tilde{h})$. This allows to close the problem. Let us define $\tilde{\tau}_b$ the bottom stress, or wall shear stress, and Γ the shape factor coefficient, or Boussinesq coefficient as:

$$\tilde{\tau}_b = \frac{1}{Re}\left(\frac{\partial \tilde{u}}{\partial \tilde{z}}\right)_b, \qquad \Gamma = \frac{\tilde{h}\int \tilde{u}^2 d\tilde{z}}{(\int \tilde{u} d\tilde{z})^2}. \tag{10}$$

In general, these quantities are functions of x, where the integral $\int \cdot d\tilde{z}$ is a short hand for integration from the bottom to the free surface. The main hypothesis for Saint-Venant models is to suppose that the velocity profile has always the same "shape" in the longitudinal direction $\tilde{x}$, so that Γ is supposed to be constant. The previous equations then read

$$\frac{\partial \tilde{h}}{\partial \tilde{t}} + \frac{\partial \tilde{Q}}{\partial \tilde{x}} = 0, \tag{11a}$$

$$\frac{\partial \tilde{Q}}{\partial \tilde{t}} + \frac{\partial}{\partial \tilde{x}}\left(\Gamma\frac{\tilde{Q}^2}{\tilde{h}} + \frac{\tilde{h}^2}{2}\right) = -\tilde{h}\frac{\partial \tilde{z}_b}{\partial \tilde{x}} - \tilde{\tau}_b \tag{11b}$$

in which $\tilde{\tau}_b$ has still to be written as a function of $(\tilde{Q}, \tilde{h})$ and Γ is a constant. If one considers a steady viscous homogeneous flow in $\tilde{x}$ with a constant pressure gradient, the solution of (5a)–(5c) is a half-Poiseuille (Nusselt film solution): the shape is $\tilde{u}_p = \frac{3}{2}\tilde{z}(2-\tilde{z})$. This profile has the following characteristics: $\int_0^1 \tilde{u}_p d\tilde{z} = 1$ and $\int_0^1 \tilde{u}_p^2 d\tilde{z} = \frac{6}{5}$, and the slope at the wall is $\partial \tilde{u}_p/\partial \tilde{z}|_0 = 3$. This gives the final closure (Boussinesq and friction coefficients) for laminar flows:

$$\Gamma = \frac{6}{5} \text{ and } \tilde{\tau}_b = \frac{3}{Re}\frac{\tilde{Q}}{\tilde{h}^2}.$$

For turbulent flows, an heuristic approach is necessary. In this framework, equations have to be meant as statistical ones, and hence $\tilde{Q}, \tilde{h}$ represent the statistical averages over many realizations of the flow [50]. Moreover, since the higher the Re number the flatter the velocity profile, it is usually assumed to be a simple plug-flow, which corresponds to $\Gamma = 1$. Furthermore, following Prandtl analysis, the friction is taken to be proportional to the square of the mean velocity $(\tilde{Q}/\tilde{h})$ with a coefficient $c_f/2$ proportional to $Re^{-1/4}$ (and maybe function of the bottom rugosity, see Schlichting's book [49]). This gives the following closure for turbulent flows:

$$\Gamma = 1 \text{ and } \tilde{\tau}_b = \frac{c_f}{2}\frac{\tilde{Q}^2}{\tilde{h}^2},$$

(see [51] for an example with a transition from one to the other model in the Shallow Water approximation).

This kind of closure deserves a critical assessment. In particular, the hypothesis underlying these closures cannot be general. For instance, Watson [28] found a laminar self-similar solution of (5a)–(5b)–(5c) with no pressure gradient (steady flow, large velocity). This solution comes from a balance between inertia and viscosity only, it gives a linear profile in x for h and a velocity profile. The associated closure is:

$$\Gamma = 1.25697 \text{ and } \tilde{\tau}_b = \frac{2.2799}{Re}\frac{\tilde{Q}}{\tilde{h}^2}.$$

This shows clearly that, in general, it is necessary to solve Eqs. (5a)–(5c) to directly compute the correct coefficients Γ and $\tilde{\tau}_b$.

(...)

4. Results

Having presented the Boundary-Layer model and the numerical scheme, this section is devoted to illustrating some numerical applications. These examples are used both to validate the method and to point out the differences with the "standard" Saint-Venant approach. In particular, the impact of the shape factor and friction coefficient which are to be closed in shallow-water approximation, are assessed. First the viscous examples of slumps by Huppert [55] and [56] are considered. In these cases, the flow is so viscous that the velocity remains always a half-Poiseuille one and the inertia is negligible in (11a)–(11b). Non-linearity is introduced afterwards in the standing jump cases [25]. Web links for the codes of most of the examples presented here are given in the Appendix. Among them one of the example of [11–13] is reproduced.

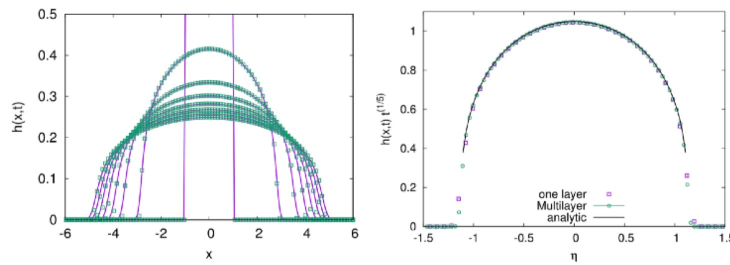

Fig. 3. Collapse of a viscous flow on a flat surface. Left: at $\tilde{t} = 100, 300, 500 \ldots 1500$ plot of $\tilde{h}(\tilde{x}, \tilde{t})$ for Saint-Venant (solid purple line) and multilayer resolution (green □). The initial height is $\tilde{h}(\tilde{x}, 0) = 1$ for $-1 < \tilde{x} < 1$, and surface $\int_0^1 \tilde{h}(\tilde{x}, 0)d\tilde{x} = 2$. Right: plot for $\tilde{t} > 500$ of $\mathcal{H}(\eta) = \tilde{t}^{1/5}\tilde{h}(\tilde{x}, \tilde{t})$ as function of $\eta = \tilde{x}/\tilde{t}^{1/5}$ with Saint-Venant (purple □) and multilayer resolution (green ○), and analytical (solid black line), which is here numerically $(0.9(1.28338 - \eta^2))^{1/3}$.

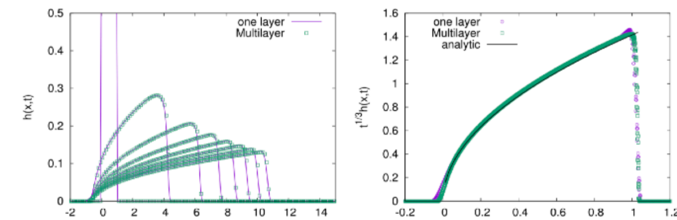

Fig. 4. Collapse of a viscous flow along a slope. (left) at $\tilde{t} = 100, 300, 500 \ldots 1500$ plot of $\tilde{h}(\tilde{x}, \tilde{t})$ for Saint-Venant (purple solid line) and multilayer resolution (empty green square). The initial height is $\tilde{h}(\tilde{x}, 0) = 1$ for $0 < \tilde{x} < 1$, and surface $\int_0^1 \tilde{h}(\tilde{x}, 0)d\tilde{x} = 1$. (right) plot for $\tilde{t} > 500$ of $\mathcal{H}(\eta) = \tilde{t}^{1/3}\tilde{h}(\tilde{x}, \tilde{t})$ as a function of $\eta = \tilde{x}/\tilde{t}^{1/3}$ with Saint-Venant (empty purple circle), multilayer resolution (empty green square), and analytical square root self-similar solution. Here $\alpha = 1/2$, so that $\tilde{x}_f = (3^{2/3}/2)\tilde{t}^{1/3}$, with $(3^{2/3}/2) \simeq 1.04$.

4.1. Stress induced flow

To validate our implementation we consider the flow of a fluid in a closed basin driven by a constant wind stress at the top (wind-driven cavity, as proposed in [57]). The action of the wind induces a stress on the free surface which causes the motion of the liquid. The value of the wind stress gives the scale of the flow. Because the fluid is confined, the only stationary solution is a steady-state recirculation inside the basin. The boundary conditions on the horizontal velocity are Neumann on the top and no-slip on the other sides. The solution for the vertical profile of the horizontal velocity at the centreline is, by symmetry:

$$\tilde{u} = \frac{\tilde{z}}{4}(3\tilde{z} - 2)$$

so that the stress at the surface is unity and the mass flow is zero. If the domain is long enough this solution is valid for a large part of the flow, except at the boundaries (left and right). We report in Fig. 2 (left) the comparison between results obtained with our solver and the analytical solution. We vary the number of layers from 4 to 32 and keep constant the horizontal resolution to 64 grid cells. We compute the norm L_1 of the error and verify that the use of the boundary condition (23) gives a second-order convergence rate while in [13] it is reported that the use of a Navier friction coefficient for the bottom condition reduce the convergence rate order from 2 to 1.7.

4.2. Viscous collapse on a plate

4.2.1. Horizontal plate

The slump of an initial heap of viscous fluid on a horizontal plate is considered. This is a double dam break viscous problem. In this flat bottom case [55], $\tilde{z}_b = 0$, the pressure gradient balances friction so that from (11b) one obtains $\tilde{Q}$, which is substituted in mass conservation (11a), and the laminar Saint-Venant equations simplify into a single evolution equation (with $k = \frac{Re}{3}$):

$$\frac{\partial \tilde{h}}{\partial \tilde{t}} - k\frac{\partial}{\partial \tilde{x}}\left(\tilde{h}^3\frac{\partial \tilde{h}}{\partial \tilde{x}}\right) = 0. \tag{26}$$

This equation has a self-similar solution $\tilde{h} = \tilde{t}^{-1/5}\mathcal{H}(\tilde{x}\tilde{t}^{-1/5})$ of the self-similar variable $\eta = \tilde{x}\tilde{t}^{-1/5}$ which turns out to be:

$$\mathcal{H}(\eta) = \frac{3^{2/3}\eta_f^{2/3}}{10^{1/3}}\left(1 - \frac{\eta^2}{\eta_f^2}\right)^{1/3} \quad \text{where } \eta_f = \frac{2^{1/5}5^{4/5}\Gamma\left(\frac{5}{6}\right)^{3/5}}{3^{2/5}\pi^{3/10}\Gamma\left(\frac{1}{3}\right)^{3/5}},$$

with Γ the Euler function, not to be confused with the Boussinesq coefficient. On Fig. 3, an example of the full resolution of (12a)–(12b) is presented, showing some profiles of $\tilde{h}(\tilde{x}, \tilde{t})$ during the collapse. The same curves are plotted in self-similar variables demonstrating the collapse of all the rescaled heights on the master curve $\mathcal{H}(\eta)$ with the self-similar variable η. The solution of (11a)–(11b) gives almost the same result, as well as the direct resolution of Eq. (26) (not presented here). As expected, the resolution of (12a)–(12b), after a short transient phase, gives the computed values:

$$\frac{\tilde{h}\int \tilde{u}^2 d\tilde{z}}{(\int \tilde{u}d\tilde{z})^2} \simeq 1.2 \text{ and } \frac{\partial \tilde{u}}{\partial \tilde{z}}_0\frac{\tilde{h}^2}{\tilde{Q}} \simeq 3.0$$

which are the half-Poiseuille Nusselt values.

4.2.2. Inclined plate

An initial heap of viscous fluid is released on an inclined plate with a constant slope [56]. In this case, pressure gradient and inertia are negligible, there is only a balance between the projection of gravity along the plate and the viscous friction. The laminar Saint-Venant equations simplify into a single evolution equation: ($k = Re\frac{\partial \tilde{z}_b}{\partial \tilde{x}}$):

$$\frac{\partial \tilde{h}}{\partial \tilde{t}} - k\tilde{h}^2\frac{\partial \tilde{h}}{\partial \tilde{x}} = 0.$$

This equation has a self-similar solution $\tilde{t}^{-1/3}\mathcal{H}(\tilde{x}/\tilde{t}^{1/3})$ which turns out to be:

$$\mathcal{H}(\eta) = \sqrt{(\eta)/k}.$$

so that for a given initial mass $A_0 = \int_0^{\tilde{x}_1} h(\tilde{x}, 0)d\tilde{x}$, the flow spreads up to $\tilde{x}_f = (\frac{9A_0^2k\tilde{t}}{4})^{1/3}$ and

$$\tilde{h} = \tilde{t}^{-1/3}\sqrt{((\tilde{x})\tilde{t}^{-1/3})/k} = \sqrt{\frac{\tilde{x}}{k\tilde{t}}}.$$

Huppert's resolution to find the solution is based on the method of characteristics. It is not based on this self-similar analysis. See on Fig. 4 the numerical resolution and some profiles at different times. Again, numerical resolution of (12a)–(12b), after a short transient phase, gives the half-Poiseuille Nusselt profile. The self-similar solution is obtained (Fig. 4) for large times for the Saint-Venant (Eqs. (11a)–(11b)) and the multilayer resolution of RNSP (Eqs. (12a)–(12b)). The profiles are plotted in self-similar variables showing the collapse of all the rescaled heights on the master curve $\mathcal{H}(\eta)$ with the self-similar variable η.

Note that a small time step Δt (small CFL condition) is needed in the Saint-Venant approximation, in order to prevent an artificial numerical slip of the bump. Moreover, with the Saint-Venant model, a spurious small numerical overshoot appears at the shock, which is also present in the multilayer solution, when N is small.

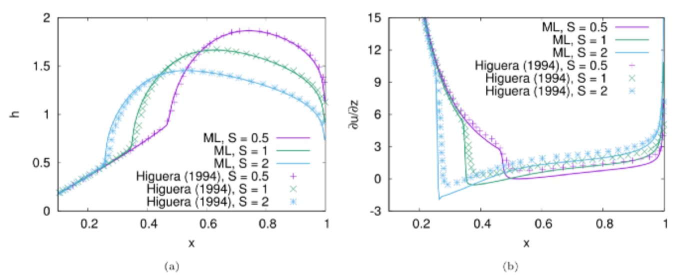

Fig. 6. Comparison of the liquid depth $\tilde{h}$ (a) and skin friction (b) solution of Eq. (27) with the data from [25]. Multilayer solver (ML) in "bar" variables (Froude number is $S^{-1/2}$): $S = 0.5$ solid purple line, $S = 1$ solid green line, $S = 2$ solid blue line. Data from [25]: $S = 0.5$ red +, $S = 1$ green ×, $S = 2$ blue ∗.

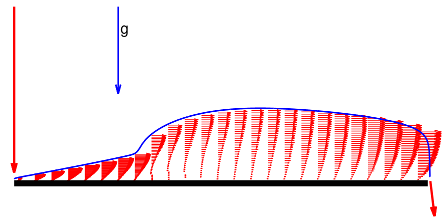

Fig. 5. Sketch of the flow, the free surface is in blue, longitudinal velocity profiles in red. The fluid is falling on the left (represented by the long vertical arrow) and turns to be parallel to the plate. A thin supercritical layer grows gently. At the end of the plate, fluids falls down. A jump in the height of the free surface appears, the flow slows down across this abrupt variation. (For interpretation of the references to colour in this figure legend, the reader is referred to the web version of this article.)

4.3. Hydraulic jumps on flat surfaces

The previous two examples were relevant for the viscous and the topographic terms. In this section, we show the application of the proposed model to the study of a standing jump. This is a particularly interesting case where all the terms, inertia, viscosity, pressure gradient and topography are important (dominant balance).

4.3.1. Hydraulic jump on a horizontal surface

First the application of the proposed multilayer model is used to study a standing jump problem previously analysed by [25]. The flow is sketched in Fig. 5. A vertical 2D jet, not described in the thin layer approximation, with flow rate Q_0, impacts at the centre of a plate of length $2L$ (only one half is presented). At the beginning of the plate, the flow is very fast and supercritical. Then, due to the fact that the flat plate is of finite extent, and due to viscous effects, a deceleration occurs downstream. Hence, a jump connects a region of fast flow (supercritical) to another of slower velocity (subcritical). This decrease is due to viscosity so that for this configuration $Re = 1$ which gives $L = h_0(c_0h_0)/\nu_0$. This problem has been described, for a plane surface using the steady RNSP model [25], and in the axi-symmetric case [26], yet using a different scaling of the equations. Instead of scaling velocity with c_0, Higuera uses Q_0/h_0 were Q_0 is the flow rate. The steady equations obtained in [25] are therefore

$$\frac{\partial \bar{u}}{\partial \bar{x}} + \frac{\partial \bar{w}}{\partial \bar{z}} = 0, \ \bar{u}\frac{\partial \bar{u}}{\partial \bar{x}} + \bar{w}\frac{\partial \bar{u}}{\partial \bar{z}} = -S\frac{\partial \bar{h}}{\partial \bar{x}} + \frac{\partial^2 \bar{u}}{\partial \bar{z}^2} \text{ given } \int_0^{\bar{h}} \bar{u}d\bar{z} = 1, \tag{27}$$

with this choice the Froude number is $S^{-1/2}$. With our choice, those equations are:

$$\begin{aligned} &\frac{\partial \tilde{u}}{\partial \tilde{x}} + \frac{\partial \tilde{w}}{\partial \tilde{z}} = 0, \\ &\frac{\partial \tilde{u}}{\partial \tilde{t}} + \frac{\partial \tilde{u}^2}{\partial \tilde{x}} + \frac{\partial \tilde{u}\tilde{w}}{\partial \tilde{z}} = -\frac{\partial \tilde{h}}{\partial \tilde{x}} + \frac{\partial^2 \tilde{u}}{\partial \tilde{z}^2} \text{ given } \int_0^{\tilde{h}} \tilde{u}d\tilde{z} = \tilde{Q}. \end{aligned} \tag{28}$$

It is straightforward to see that the relation between S and $\tilde{Q}$ is: $S^{-1/2} = \tilde{Q}^{5/2}$.

For steady flow $\tilde{Q}$ is indeed constant, then the value of $\tilde{Q}^{5/2}$ is a global Froude number.

Let us begin with analysing some asymptotic behaviours, for which analytical results can be obtained. For small S, or large $\tilde{Q}$, the pressure gradient is negligible, from Eq. (28) one obtains the Watson self-similar solution (steady flow, balance between inertia and viscosity) $u_w = \frac{1}{x}f(\eta)$ with $\eta = y/x$. The function f is solution of the equation $f'' = -f^2$ with $f(0) = 0, f'(H_w) = 0$ for a unit flow rate $\int_0^{H_w} f(\eta)d\eta = 1$. After solving the equation, one finds: $H_w = 1.8138$, $f(H_w) = 0.8964$ and $f'(0) = 0.693$. So that $\tilde{h}(\tilde{x}) = 1.8138\tilde{x}$. The already mentioned shape factor is $\Gamma = H_w\frac{\int_0^{H_w} f(\eta)^2d\eta}{(\int_0^{H_w} f(\eta)d\eta)^2} = 1.25697$, the shear is $\tau_b = f'(0)H_w^2 = 2.2799$.

Another limit of Eq. (28) may be obtained for large S, or small $\tilde{Q}$, when the pressure gradient is no more negligible, but inertia is now negligible, one obtains the Poiseuille solution (balance between pressure gradient and viscosity).

$$\tilde{u} = -\tilde{h}^2\frac{\partial \tilde{h}}{\partial \tilde{x}}\frac{(\tilde{y})}{2\tilde{h}}(2 - \frac{(\tilde{y})}{\tilde{h}}), \quad \tilde{Q} = -\frac{\tilde{h}^3}{3}\frac{\partial \tilde{h}}{\partial \tilde{x}}$$

so that one can solve the equation for $\tilde{h}(\tilde{x})$, and as a small height (even 0) is given at the boundary condition, we neglect it and obtain as an approximation of the surface position for small flow rate near the output:

$$\tilde{h}(\tilde{x}) = (12\tilde{Q})^{1/4}(1 - \tilde{x})^{1/4},$$

the shape factor is $\Gamma = \frac{6}{5}$ and shear is $\tilde{\tau}_b = 3$.

We present here the numerical results for the full problem. The system of equations is solved using $\tilde{Q}$ (or S) as a parameter. A first flat profile is imposed at the input at $\tilde{x} > 0$ on a small given height (say 0.1) compatible with Watson's solution. At the outlet a zero Neumann boundary condition is imposed on the velocity and a zero depth, $\tilde{h} \to 0$. The simulations have been performed using 256 points in the horizontal direction and 30 layers in the vertical direction. These values have been chosen checking the convergence both on the thickness of the hydraulic jump, influenced by the horizontal resolution, and on the skin friction which is affected by the number of layers.

Fig. 6 shows a comparison of the free surface profile and the skin friction (resp. $\bar{h}(\bar{x})$ and $\partial\bar{u}/\partial\bar{z}|_0$), for different values of S, between the solution obtained with the proposed solver, written in "bar" variables, Eq. (28), and the data from [25]. The agreement is quite good.

5. Conclusions

(...)

This work presents a reduced set of Navier–Stokes equations leading to a kind of Prandtl system of equations (RNSP equations), obtained through the asymptotic thin-layer expansion. These are the Prandtl equations with different boundary conditions (Schlichting [49]) and they have already been derived on more phenomenological grounds [24–26]. These thin-layer incompressible equations assume hydrostatic pressure by construction. If they are integrated over the depth of fluid, they give the Saint-Venant equations (or Shallow Water equations). In these reduced Navier–Stokes equations no hypothesis is made about the velocity profile, which is a result of the computations, whereas in the Saint-Venant equations a closure hypothesis is necessary.

• correction Ex 2

2.1 Newton's law for a mass falling in gravity with viscous friction is

$$m\frac{d^2y}{dt^2} = -mg - 6\pi\mu R\frac{dy}{dt}.$$

We have for sure a competition between free fall mg and viscous drag. A natural velocity is the Stokes velocity $V_s = mg/(6\pi\mu R)$, this is the terminal chute velocity. We define the scales $y = Y\bar{y}$ and $t = \tau\bar{t}$, we have :

$$\frac{V_s}{g}\frac{Y}{\tau^2}\frac{d^2\bar{y}}{d\bar{t}^2} = -V_s - \frac{Y d\bar{y}}{\tau d\bar{t}},$$

hence we take $\frac{Y}{\tau} = V_s$ and we identify $\varepsilon = V_s/(g\tau)$, so that we obtain the following ODE

$$\varepsilon\frac{d^2\bar{y}}{d\bar{t}^2} = -1 - \frac{d\bar{y}}{d\bar{t}}.$$

Boundary condition are same : $\bar{y}(0) = 0$ and $\bar{y}'(0) = 0$. Indeed, the ratio $\frac{V_s}{g\tau}$ is small if velocity scale $g\tau$ of free fall is large compared to the Stokes velocity. Or when the time scale τ compared to the time scale V_s/g is large. Or if the mass is small, or if viscosity is small.....

2.2 Problem singular for small ε, indeed, if we put $\varepsilon = 0$, we have 2 BC, but only one degree of derivation , $\bar{y}_{out}(0) = 0$ and $\bar{y}'_{out}(0) = 0$

$$0 = -1 - \frac{d\bar{y}_{out}}{d\bar{t}}$$

we take $\bar{y}_{out}(0) = 0$ so that $\bar{y}_{out}(t) = -\bar{t}$, the problem is in $\bar{t} = 0$ where $\bar{y}_{out}(0) = -1 \neq 0$

2.3 So, as we have identified a problem at small time scale, near the origin, we change the scale of time $\bar{t} = \tau_\varepsilon\tilde{t}$ and space $\bar{y} = \nu_\varepsilon\tilde{y}$

$$\varepsilon\frac{\nu_\varepsilon d^2\tilde{y}}{\tau_\varepsilon^2 d\tilde{t}^2} = -1 - \frac{\nu_\varepsilon d\tilde{y}}{\tau_\varepsilon d\tilde{t}}$$

A full dominant balance gives $\nu_\varepsilon = \tau_\varepsilon$ and $\varepsilon\frac{\nu_\varepsilon}{\tau_\varepsilon^2} = 1$ so that $\nu_\varepsilon = \tau_\varepsilon = \varepsilon$.

The problem is in the new small scales :

$$\frac{d^2\tilde{y}}{d\tilde{t}^2} = -1 - \frac{d\tilde{y}}{d\tilde{t}}, \text{ 2 BC : } \quad \tilde{y}(0) = 0, \;\; \tilde{y}'(0) = 0$$

It is no more singular, the solution is $\tilde{y} = -\tilde{t} + A + Be^{-\tilde{t}}$ with BC in 0 gives $0 = -0 + A + B$ and $\tilde{y}'(0) = 0$ which give $0 = -1 + 0 - B$ hence :

$$\tilde{y} = 1 - \tilde{t} - e^{-\tilde{t}} \text{ and } \tilde{y}' = -1 + e^{-\tilde{t}}.$$

There is no need to match at this order, matching will appear at next order. Note the matching on velocity is verified

$$\lim_{\tilde{y}\to\infty}(\frac{\varepsilon d\tilde{y}}{\varepsilon d\tilde{y}}) = \lim_{\bar{t}\to 0}(\frac{d\bar{y}}{d\bar{t}}).$$

As when $\tilde{y} \to \infty$ then $\tilde{y} \sim -1 + \tilde{t}$ shows that the displacement induced at small time is of order ε. This will be used at next order....

++

2.4

The full solution of the problem is

$$\bar{y} = \varepsilon - \bar{t} - \varepsilon e^{-\bar{t}/\varepsilon}$$

we see that indeed, for $\varepsilon \to 0$

$$\bar{y} = -\bar{t}$$

as seen for the external solution, we see as well the ε small displacement induced by the small time, $\bar{t} = \varepsilon\tilde{t}$, corresponding to the interanl problem :

$$\varepsilon\tilde{y} = \varepsilon - \varepsilon\tilde{t} - \varepsilon e^{-\tilde{t}}$$

Finally, note that if we take very small time

$$\bar{y} = \varepsilon - \bar{t} - \varepsilon(1 - \bar{t}/\varepsilon + \bar{t}^2/\varepsilon^2/2 ... = -\bar{t}^2/\varepsilon/2 = -\varepsilon\tilde{t}^2/2 + ...$$

this is the free fall.

```
DSolve[{eps y''[t] == -y'[t] - 1, y[0] == 0, y'[0] == 0}, y[t], t]
Expand[E^(-(t/eps)) (-eps + E^(t/eps) eps - E^(t/eps) t)]

DSolve[{ y''[t] == -y'[t] - 1, y[0] == 0, y'[0] == 0}, y[t], t]
```

- **correction Ex 3**

ε is the small parameter : $t_0 = t$ and $t_1 = \varepsilon t$...

$$\cos t - t/4 \cos t$$

$$y_0'' + y_0 = (2B' + B/2)\cos t_0 + -(2A' + A/2)\cos t_0$$

secular terms ... solution

$$e^{-t_1/4}\cos t$$

$$\Delta = -\varepsilon/4 \pm i\sqrt{1 - \varepsilon^2/16}$$

- **correction Ex 4**

- with $\delta = \varepsilon$, the eikonal $S_0' = -2$ hence the solution is $y(x) = e^{-2x/\varepsilon}$. c'est exactement la solution exacte !

correction Ex 2

Exactly the curse with cos,

```
In[18]:= Simplify[DSolve[y''[t] + y[t] == 2 Sin[t] , y[t], t ]]

Out[18]= {{y[t] -> (-t + C[1]) Cos[t] + 1/2 (1 + 2 C[2]) Sin[t]}}
```

$y_0 = \cos(t)$ and $y_1 = -t\cos(t)$.

so that the solution is $y = e^{-t_1}\cos(t_0)$

```
se = DSolve[{y''[t] + y[t] == -2 e y'[t], y[0] == 1, y'[0] == 0},
   y[t], {t, 0, 1}];
Plot[{0, y[t] /. se /. e -> .25, Exp[-t .25], y[t] /. se /. e -> .125,
   Exp[-t .125], y[t] /. se /. e -> .05, Exp[-t .05]}, {t, 0, 4 Pi},
 Frame -> True, FrameLabel -> {"t", "y(t)"}]
```

```
se = DSolve[{e u''[y] + u'[y] + e u[y] == (1 + y)/2, u[1] == 1,
    u[0] == 0}, u[y], {y, 0, 1}];
s = DSolve[{u'[y] == (1 + y)/2, u[1] == 1}, u[y], {y, 0, 1}];
Plot[{0, u[y] /. se /. e -> .25, u[y] /. se /. e -> .125,
  u[y] /. se /. e -> .05 u[y] /. se /. e -> .025, u[y] /. s}, {y, 0,
  1}, Frame -> True, FrameLabel -> {"x", "u(x)"}]
```